Photoluminescence and photoluminescence excitation study of $CuGaTe_2$

J. Krustok[a)]
Tallinn Technical University, Ehitajate tee 5, Tallinn, EE0026, Estonia

H. Collan and K. Hjelt[b)]
Optoelectronics Laboratory, Helsinki University of Technology, P.O. Box 3000, FIN-02015, Espoo, Finland

M. Yakushev, A. E. Hill, and R. D. Tomlinson
Department of Physics, University of Salford, Salford, M5 4WT, United Kingdom

H. Mändar
Tartu University, Tähe 4, Tartu, EE2400, Estonia

H. Neumann
E.O.M.C. Fritz-Siemon-Str. 26/111, D-04347 Leipzig, Germany

(Received 16 February 1998; accepted for publication 19 March 1998)

Photoluminescence (PL) and photoluminescence excitation measurements over a temperature range 12 K$<T<$300 K on high quality $CuGaTe_2$ crystals grown by the vertical Bridgman method were completed. The whole PL spectrum consists of two regions. The first region includes PL bands E_1 at 1.431 eV, E_2 at 1.426 eV, and E_3 at 1.417 eV, together with their phonon replicas while in the second region we have a PL band D_0 at 1.338 eV with its well-resolved LO-phonon replicas ($\hbar\omega_{LO}=26.5$ meV). All these PL bands appear to be at higher energy than the lowest (fundamental) band gap energy E_g^A. The possible origin of observed PL bands is discussed. © *1998 American Institute of Physics.* [S0021-8979(98)04712-4]

I. INTRODUCTION

Over recent years the physical properties of I–III–VI_2 semiconductors have been studied intensively because of their promising potential as solar cell materials. However, the optical properties of the tellurides of this group, such as $CuGaTe_2$, are still relatively poorly understood.

It is known, that $CuGaTe_2$ has usually a p-type conductivity and a direct band gap $E_g=1.22-1.24$ eV at room temperature.[1–6] Although also some data on the low-temperature optical properties near the fundamental edge of $CuGaTe_2$ have been reported, practically no information is available about the defect levels and luminescence measurements in this material. It is known, that the photoluminescence (PL) spectroscopy can be a valuable tool to study defect levels, but as far as we know, no low-temperature ($T<77$ K) PL measurements on $CuGaTe_2$ have been done so far. However, PL measurements done earlier at 77 K have shown that in $CuGaTe_2$ samples very interesting features can be seen.[7,8] In the present article we report for the first results of detailed low-temperature PL studies of $CuGaTe_2$ single crystals grown by the vertical Bridgman method. These results reveal several novel features and clearly point the way forward to a more detailed investigation.

II. GROWTH AND PROPERTIES OF THE $CuGaTe_2$ SINGLE CRYSTALS

A polycrystalline ingot of the near stoichiometry $CuGaTe_2$ composition was synthesized from individual elements with 99.999% purity in a vacuum sealed quartz tube with diameter 10 mm. The melting point and phase transition temperatures as well as the phase diagram were taken from Ref. 9. The ampoule with about 25 g charge was heated up to 1000 °C and cooled in horizontal position in order to prereact the components. After cooling it down to the room temperature the ampoule was introduced into a two zone furnace for growth by the vertical Bridgman technique.[10]

During the growth process the ampoule was held in a quartz holder on the top of a porcelain rod in the center of the furnace tube, without touching the wall, in order to avoid sudden vibrations during the movement of the furnace. The prereacted material was melted at 1000 °C and held at this temperature for 6 h in the upper, hot zone of the furnace. Next, the ampoule was translated through a temperature gradient of about 0.5 °C/cm by moving the furnace up with the speed of 2 cm/day. The solidified material was cooled at 1 °C/h rate through the phase transition down to 600 °C. Below this temperature the ampoule was cooled with a gradually increasing rate. The fabricated ingot was about 6 cm long and consisted of several grains with lengths from 0.5 to 1.5 cm. One of these grains taken from the middle part of the ingot, was sliced perpendicular to the growth direction into full circular shaped crack free samples, each about 1.5 mm thick. Slices, polished with 3 and 1 μm diamond paste, and then etched for 2 min in a 1% Br-methanol solution, were analyzed by the energy dispersive spectroscopy (EDS) technique. The elemental composition was found to be in good agreement with the melt composition: 23.43 at. % Cu, 24.63 at. % Ga, and 51.94 at. % Te. The resulting $CuGaTe_2$ crystal had a p-type conductivity as proved by a thermal probe measurements.

a)Electronic mail: krustok@cc.ttu.ee
b)Present address: Electronic Instrumentation Lab., DIMES, Delft University of Technology, Mekelweg 4, 2628 CD Delft, The Netherlands.

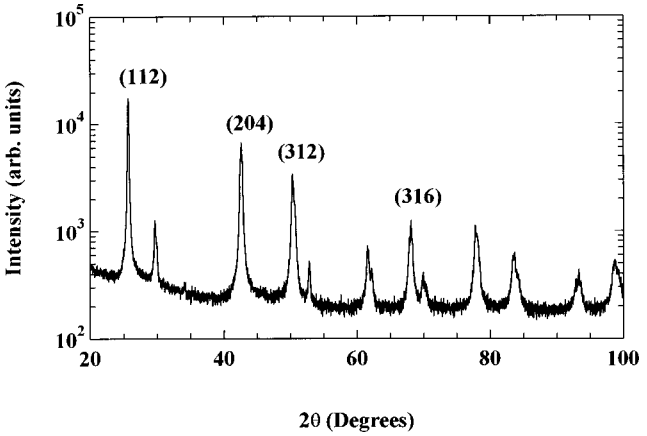

FIG. 1. XRD profile of $CuGaTe_2$ powder sample.

An electron channeling pattern (ECP) was obtained from various points on cleaved and polished-etched surfaces. The fact that ECP over the surface yielded the same pattern, was taken as an evidence that the samples are single crystals. Because the contrast of an ECP comes from the near surface layer, the perfection of the crystalline lattice can be assessed from the contrast of the ECP. Polished and unetched surface yielded no ECP. Etched surface ECP usually gave worse contrast than ECP from cleaved surfaces. Because of this a cleaved crystal surface was used for the optical measurements.

X-ray diffraction measurements of the powdered $CuGaTe_2$ crystal were performed and data were collected using a standard Bragg–Brentano powder diffractometer (DRON-1) with vertical axes, 180 mm radius, working at 30 kV and 20 mA. Cu $K\alpha$ radiation ($\lambda=1.5406$ Å) was collimated with Soller slits (aperture 2.5°) and a 1 mm divergence slit. Soller slits (aperture 2.5°) in the diffracted beam, a 0.03 mm Ni filter, a 0.25 mm receiving slit, and a scintillation detector were used in a step-scanning mode (0.02° of 2Θ in 5 s) for the angular range 2–100° of 2Θ.

The software system AXES[11] was used for peak detection, fitting with Pearson VII type function and search/match in the ICDD PDF-2 database. Program LSUCRE was used for the cell parameter refinement (calibration with a standard material was not used).

X-ray diffraction pattern showed 26 peaks in the 2Θ range of 20–100°, see Fig. 1. Pattern search/match on the ICDD database PDF-2 identified with figure-of-merit FOM $=6.9$ all belonged to $CuGaTe_2$ (PDF File No. 34-1500), see Table I. One peak (No. 5 in Table I) with hkl$=(115)$ was not found in the experiment. This can be explained by very low intensity of this peak $I<1\%$. Relatively large differences between the experimental and the PDF-2 data peak intensities of some peaks (e.g., 220, 204, 404, 408) can be explained by texture effects in the sample. The powder sample, prepared for diffraction, was displayed by a simple optical reflection as a few individual small grains on the surface. The preferred orientation is probably close to the direction (211) because the experimental peaks from the planes close to 112 (e.g., 116, 224, 316, 228) have a measured intensity equal or even higher compared with the peak intensities in PDF-2.

TABLE I. Comparison of the experimental sample diffraction data of $CuGaTe_2$ with the data in the database PDF-2.

	Sample data			PDF-2 (No. 34-1500)				
No.	2Θ	d,Å	I_{area},%	d,Å	I,%	h	k	l
1	25.648	3.47	100	3.469	100	1	1	2
2	29.635	3.012	6.3	3.009	9	2	0	0
3	29.888	2.987	2.2	2.985	2	0	0	4
4	34.147	2.624	0.3	2.626	1	2	1	1
5	missing			2.215	1	1	0	5
6	42.429	2.129	26.9	2.128	45	2	2	0
7	42.615	2.12	46.1	2.12	80	2	0	4
8	50.256	1.814	31.9	1.814	40	3	1	2
9	50.604	1.802	10.6	1.802	12	1	1	6
10	52.779	1.733	2.3	1.733	3	2	2	4
11	61.562	1.505	5.7	1.506	8	4	0	0
12	62.142	1.493	2.4	1.492	1	0	0	8
13	67.834	1.38	6.6	1.381	7	3	3	2
14	68.109	1.376	11.9	1.376	11	3	1	6
15	69.81	1.346	1.1	1.346	2	4	2	0
16	69.968	1.344	1.8	1.344	4	4	0	4
17	70.401	1.336	1.1	1.337	<1.0	2	0	8
18	77.793	1.227	11.9	1.227	12	4	2	4
19	78.193	1.221	12.3	1.222	4	2	2	8
20	83.381	1.158	4.7	1.158	5	5	1	2
21	83.674	1.155	3.6	1.155	4	5	0	3
						3	3	6
22	84.2	1.149	3.7	1.149	2	1	1	10
23	92.756	1.064	2.2	1.064	3	4	4	0
24	93.293	1.059	5.6	1.059	11	4	0	8
25	98.467	1.017	4.5	1.017	4	5	3	2
26	98.739	1.015	3.5	1.015	5	5	1	6
27	99.26	1.011	3.1	1.011	3	3	1	10

The cell parameter refinement gave for $a=6.0192(4)$ and $c=11.934(3)$ Å which is in good agreement with data stored in PDF-2 [$a=6.021(2)$ and $c=11.937(5)$ Å].

III. OPTICAL MEASUREMENTS

The PL measurements were carried out using the 488 nm line of an Ar^+-ion laser or Ti-sapphire laser as the excitation source. The sample was mounted on a cold finger of a closed-cycle cryostat which can be cooled down to 10 K. The luminescence radiation was analyzed by a 0.5 m grating monochromator SPEX 1870 and an LN_2 cooled Ge detector using lock-in technique.

The slits of the monochromator usually had the width corresponding to a spectral resolution of 0.45 nm over the measuring range, translating to an energy resolution better than 1 meV. For the purpose of the analysis, the emission spectra were corrected for grating efficiency variations and for the spectral response of the detector, measured separately.

For the photoluminescence excitation (PLE) measurements a tunable Ti-sapphire laser was used for the excitation. The detector monochromator was tuned to the peak of the D_0 PL band, $E=1.338$ eV at 12 K. The resulting PLE spectra were also corrected for the laser emission efficiency variations.

IV. RESULTS AND DISCUSSION

A typical PL spectrum of a $CuGaTe_2$ sample at 11.5 K is shown in Fig. 2. The whole spectrum consists of two regions.

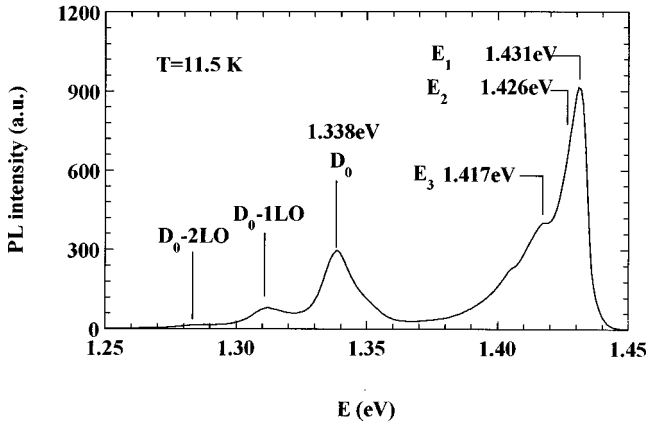

FIG. 2. A typical PL spectrum of the $CuGaTe_2$ single crystal studied.

The first region at the upper band edge includes PL bands E_1 at 1.431 eV, E_2 at 1.426 eV, and E_3 at 1.417 eV, together with their phonon replicas while in the second region we have a PL band D_0 at 1.338 eV with its well-resolved LO-phonon replicas. The separation between these phonon replicas gives us a LO-phonon energy $\hbar\omega_{\mathrm{LO}}=26.5$ meV. As is usual, we assume here that the intensity of the D_0 peak and its phonon replicas follow a Poisson distribution

$$I(n)=I_0 e^{-S}\frac{S^n}{n!}. \tag{1}$$

Here S is the Huang–Rhys coupling parameter and I_0 is a scaling constant. By fitting the measured spectra to Eq. (1) we can see that the S parameter has a value $S\approx 0.29$. We feel that it is important to observe that the high energy tail of the D_0 band has a closely exponential shape while other PL bands can be fitted with Gaussian shape.

Excitation with varying laser power showed that the D_0 band did not shift or change its shape with laser power. At the same time various changes take place in the upper edge emission region, see Fig. 3. The intensity of the E_1 PL band increases with excitation intensity more rapidly ($I\sim I_{\mathrm{exc}}^{1.3}$) than the intensity of other bands in this region. Additionally there is a little shift of E_2 and E_3 PL bands towards higher energies with excitation intensity.

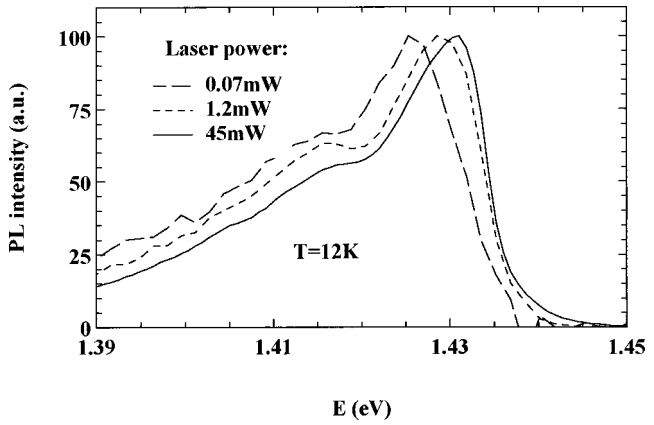

FIG. 3. Normalized PL spectra of the $CuGaTe_2$ crystal as a function of excitation intensity.

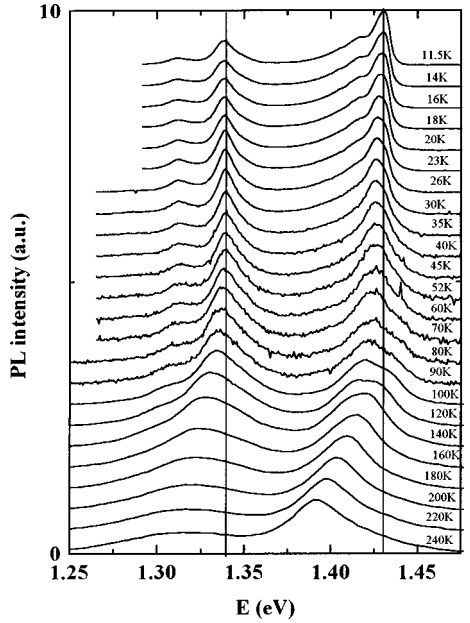

FIG. 4. Normalized PL spectra of the $CuGaTe_2$ crystal, shown as a function of temperature.

The general temperature dependence of PL spectra is shown in Fig. 4. Although the precise spectral features are not discernible by naked eye only, several conclusions can be drawn. At low temperatures the upper edge emission is dominated by the E_1 band. This band vanishes approximately at 40 K leaving the E_2 band to be the most intense. Starting from 80 K a new band appears at the higher energy side of the E_2 band and this feature dominates the edge emission region at higher temperatures ($T>140$ K). The high-energy side of this band decreases exponentially according to the $\exp[-(E-E_g)/kT]$ relation. This is a typical feature for band-to-band recombination, with the hole mass m_h much larger than the conduction band electron mass m_e, and therefore it is reasonable to identify this band as the BB band. At the same time the high-energy side of the D_0 band decreases according to $\exp[-(E-E_g')/2kT]$. This result can be explained, if we suppose, that the recombination is also a band-to-band type, but with relatively light holes such that $m_h\sim m_e$.

In order to study the temperature quenching of PL bands we first divided spectra into two regions, the D band and the edge emission (EE) band, and then plotted the integrated intensity of each of these versus temperature, see Fig. 5.

It is obvious from Fig. 5 that both of the bands show multiple quenching processes. Therefore we used the following semiempiric equation to fit the experimental data plotted in Fig. 5:

$$\Phi(T)=\sum_n \frac{I_{0n}}{1+\beta_n \exp\left(-\dfrac{E_{Tn}}{kT}\right)}. \tag{2}$$

The D and EE bands were thus fitted with two and three different quenching processes, respectively, and the parameters obtained are collected in Table II. The resulting $\Phi(T)$ functions of this fitting are also given in Fig. 5 as continuous

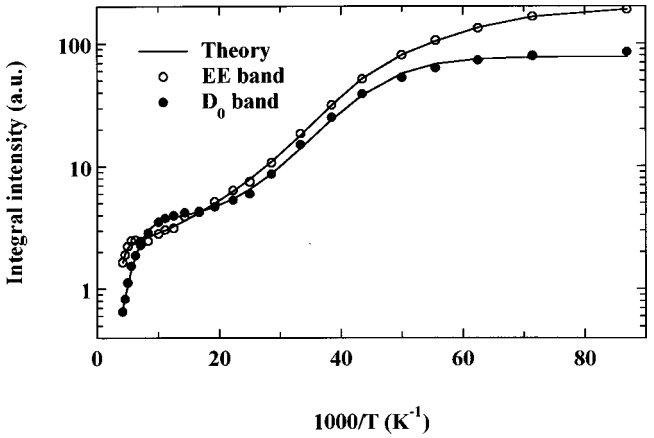

FIG. 5. Temperature dependence of integrated intensity of the D_0 and EE PL bands. Continuous curves show the result of parameter fitting to Eq. (2) with parameter values as given in Table II.

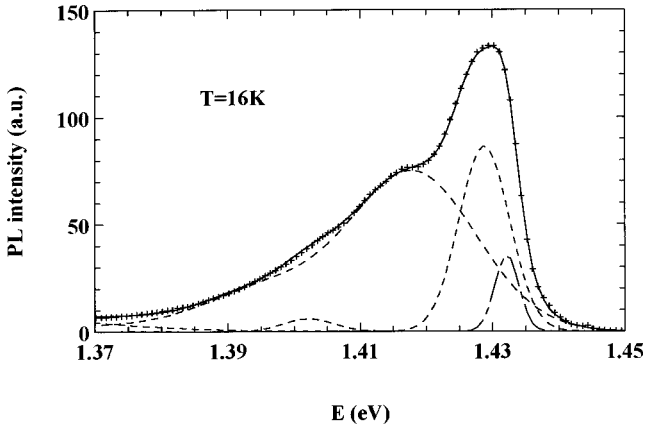

FIG. 6. Result of fitting of the EE band with Eq. (1).

lines. The fitting function used in Eq. (2) is semiempiric only; therefore it is not easy with any certainty to assign precise physical meaning to the parameters. Nevertheless, broadly speaking at least, from these data, the following conclusions can be drawn:

(1) The first stage of the EE band quenching is determined by the E_1 band with an activation energy of $E_T=8.7$ meV. Because the intensity of the E_1 band increases rapidly with laser power and because it has also a very small half-width (full width at half maximum, $W\sim5$ meV) we believe, that the E_1 band has probably an excitonic origin.
(2) The first stage of the D band quenching gives an activation energy $E_T=14$ meV and the high temperature quenching of this band has an activation energy $E_T=65$ meV. It is clear that there is a certain inconsistency between the rather ''deep'' position of this PL band and the rather ''shallow'' values of E_T and S found for this band.
(3) The second stage of quenching of the EE band is probably determined by the E_2 band, which quenches with an activation energy $E_T=22$ meV. The peak position of this band is also located about 20 meV below the ''band gap,'' the magnitude of which was determined at 11.5 K by the PLE measurements to be $E_g=1.446$ eV.
(4) The high temperature quenching of the EE band is determined by the quenching of the free carrier band to band emission, but the activation energy of this process is quite indeterminate.
(5) We were not able to find any clear-cut activation energy for the E_3 band.

TABLE II. Fitting parameters for the EE and D PL bands in $CuGaTe_2$.

Parameter	EE band	D band
I_{01}	167.8	74.7
β_1	332	1380
E_{T1} (meV)	8.7±0.3	14.0±0.7
I_{02}	28.6	3.5
β_2	51300	115
E_{T2} (meV)	22±3	65±5
I_{03}	1.5	
β_3	38000	
E_{T3} (meV)	225±30	

To obtain more information about the upper edge emission region (''E'') of our PL spectra we fitted tentatively several low temperature spectra with three different series of Gaussian bands. In each series the intensity distribution was taken from Eq. (1) and the individual bands were separated by the LO-phonon energy $\hbar\omega_{LO}=26.5$ meV. The result of one such fitting is given in Fig. 6. The fitting of various spectra showed, that at low temperature we indeed may well have three different Gaussian bands with their phonon replicas.

In Fig. 7 we present the dependence of the Huang–Rhys coupling parameter S of these bands on the zero-phonon subbands peak position as obtained from the fitting. The result is a nearly linear function which may be taken to indicate that the D band with $S\sim0.29$ would be expected to have a peak position approximately at $E=1.416$ eV. This value is very close to the peak position of the E_3 band. Therefore it is reasonable to assume that the actually observed D band at low temperature is somehow connected with the different

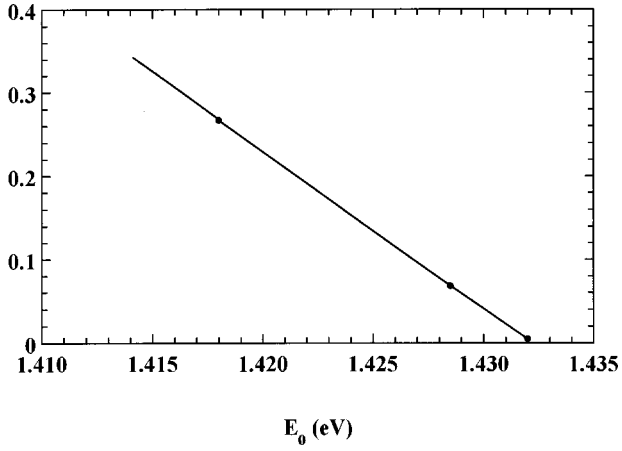

FIG. 7. The dependence of the Huang–Rhys coupling parameter S on the zero-phonon subbands peak position in $CuGaTe_2$ edge emission (E) region.

TABLE III. Reported room temperature values of the band gaps in $CuGaTe_2$.

A (eV)	B (eV)	C (eV)	References
1.22	1.28	1.42	13
1.23	1.28	1.98	12
1.23	···	1.89	14
1.24	1.27	1.86	6
1.23	1.28	1.97	5

energy gap in $CuGaTe_2$ and that the phonon replica structure may have the same basis as the E_3 band. From the difference between the peak positions of the ''theoretical'' and the measured D_0 band we are able to calculate the approximate difference between two energy gaps $\Delta E_g = 1.416 - 1.338 = 78$ meV. Although this value is rather rough, it gives us an order of magnitude for this effect—and a clue to the explanation of our results.

It is known that in $CuGaTe_2$ three different direct energy gaps, at $k=0$, may be present due to the crystal field splitting Δ_{cf} and the spin-orbit splitting Δ_{SO} of the uppermost valence band.[5,6,12–14] These gaps are usually called as A, B, and C gaps, but there is a great difference between the values of these gaps measured by different groups. Most of the experimental determinations have been done via a measurement of the absorption coefficient α as a function of energy which, unfortunately, may not necessarily give the magnitude of the optical gap unambiguously. Theoretical studies on the details of the band structure of chalcopyrite semiconductors are available[15–17] for comparison, and the fitting to experimental data has assumed that the fundamental direct gap for $CuGaTe_2$, at room temperature, is $E_g = 1.23$ eV. This implies, definitely, an $E_g(T=0\ \text{K})$ value <1.3 eV. Besides, no direct experimental data has been available about the low temperature values of the A, B, and C band gaps of this material. The previously reported room temperature values of the band gaps are collected in Table III.

As it can be seen from Table III, most groups have found for the A and B transitions nearly the same energies, but the most problematic seems to be the transition C, where reported values differ unusually.

Typical PLE spectra of the D_0 band are presented in Fig. 8. It can be seen that this PL band has an excitation mechanism through the band-to-band transition. We were able to measure PLE spectra at temperatures $T<100$ K. At higher temperatures ($T=120$–300 K) we used the peak position of the band-to-band (BB) PL band to follow the temperature dependence of the ''band gap.'' Both results were collected in Fig. 9. Above 130 K the BB band peak position changes approximately linearly with the temperature with a temperature coefficient of $dE_{\max}/dT = -3\times10^{-4}$ eV/K. This value is remarkably lower than the value $dE_g/dT = -4\times10^{-4}$ eV/K reported in Ref. 4. The temperature dependence of the band gap energy measured in Ref. 4 is also plotted in Fig. 9 together with the peak position of the D_0 PL band. As it can be seen from Fig. 9 almost all observed PL bands are at higher energy than the band gap energy E_g, which obviously corresponds to the lowest A transition. Therefore it is apparent

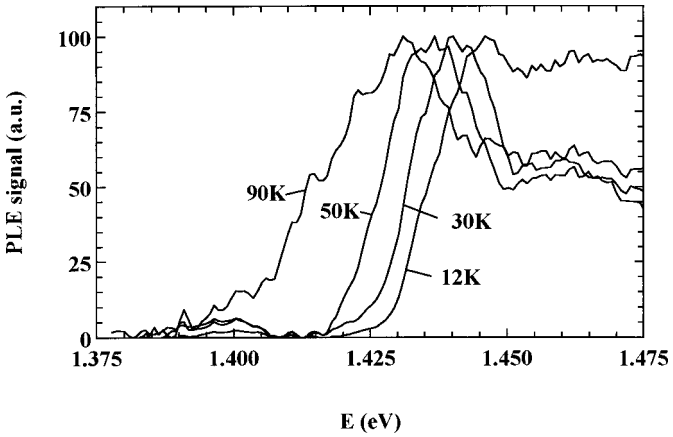

FIG. 8. Normalized PLE spectra of the D_0 PL band of $CuGaTe_2$ crystal, measured at different temperatures.

that the higher energy PL bands (''E,'' ''D'') are not connected to the transition A, at least at higher temperatures, because at low temperatures the peak position of the D_0 band is very close to the band gap (A) energy E_g^A. But the temperature dependence of the D_0 peak position is different from the temperature dependence of E_g^A found earlier and therefore it is obvious, that at higher temperatures the D_0 band is not connected with the A transition. One possibility to explain our results is to assume, that there may be present so-called B and/or C excitons. The B and C excitons from PL measurements were first detected in $CuGaS_2$ single crystals.[18] Later these excitons have been found in $CuGaSe_2$[19] and in GaN.[20] In all these materials B and C excitons were detected together with A excitons and they were always weaker than the A excitons. But in $CuGaTe_2$ it seems that PL bands corresponding to the A transition were not detected at all. Therefore it is unlikely, that our PL bands can be explained by B or C excitons. It is obvious, that the excitation energy ($\sim$2.54 eV) used in our experiment is sufficient to produce holes not only in the zone-center valence bands but also in deeper lying valence band maxima at the boundary of the Brillouin zone, and electrons can also be excited to higher conduction band minima. Thus, transitions from a higher conduction band minimum to defect states or

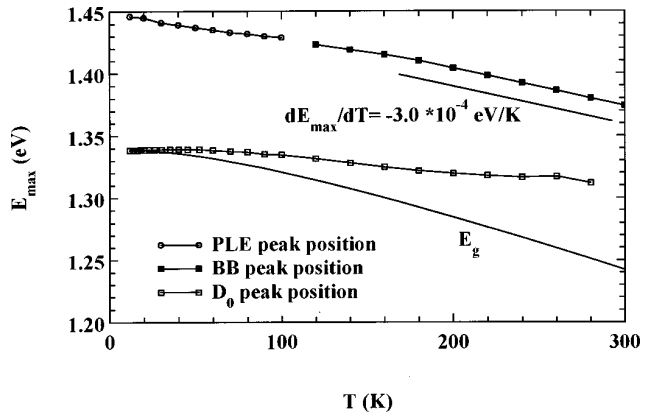

FIG. 9. Temperature dependence of the peak positions of PL and PLE bands and the band gap energy E_g (Ref. 4) in $CuGaTe_2$.

from defect states to a deeper lying valence band can also explain our PL results. Apparently further research is necessary to solve this problem.

V. CONCLUSIONS

We measured low temperature PL and PLE spectra of high quality $CuGaTe_2$ crystals grown by the vertical Bridgman method. At 12 K PL bands E_1 at 1.431 eV, E_2 at 1.426 eV, and E_3 at 1.417 eV, together with their phonon replicas and a PL band D_0 at 1.338 eV with its well-resolved LO-phonon replicas were found. The separation between these phonon replicas gives us a LO-phonon energy $\hbar\omega_{LO}=26.5$ meV. All the PL bands, observed in this work, are located at higher energies than the previously reported lowest band gap energy for $CuGaTe_2$ and, in particular, no trace was found of the expected fundamental direct gap at $E<1.3$ eV. Transitions from a higher conduction band minimum to defect states or from defect states to a deeper lying valence band may be a possible explanation of these PL bands. Observed features reveal that the further experimental work is needed to clarify the band structure of $CuGaTe_2$.

ACKNOWLEDGMENT

This work was partly supported by the Estonian Scientific Foundation Grant No. 3417.

[1] S. M. Wasim, G. Marcano, and G. Sanchez Perez, Phys. Status Solidi A **78**, 423 (1983).
[2] R. Valero, S. M. Wasim, C. Rincon, and F. Sanchez Perez, Proceedings of the 7th ICTMC, Snowmass, 1986 (unpublished), p. 115.
[3] S. A. A. Elhady, B. A. Mansour, and S. H. Moustafa, Phys. Status Solidi A **149**, 601 (1995).
[4] W. Hörig, G. Kühn, W. Möller, A. Müller, H. Neumann, and E. Reccius, Krist. Tech. **14**, 229 (1979).
[5] H. Neumann, W. Hörig, E. Reccius, H. Sobotta, B. Schumann, and G. Kuhn, Thin Solid Films **61**, 13 (1979).
[6] M. J. Thwaites, R. D. Tomlinson, and M. J. Hampshire, Inst. Phys. Conf. Ser. **35**, 237 (1977).
[7] G. Masse, K. Djessas, and F. Guastavino, J. Phys. Chem. Solids **52**, 999 (1991).
[8] G. Masse, K. Djessas, and L. Yarzhou, J. Appl. Phys. **74**, 1376 (1993).
[9] L. S. Palatnik and E. I. Belova, Izv. Akad. Nauk SSSR, Neorg. Mater. **3**, 2194 (1967).
[10] R. D. Tomlinson, Sol. Cells **16**, 17 (1986).
[11] H. Mändar, T. Vajakas, J. Felsche, and R. E. Dinnebier, J. Appl. Crystallogr. **29**, 304 (1996).
[12] M. Sesha Reddy, K. T. Ramakrishna Reddy, O. Md. Hussain, and P. J. Reddy, Thin Solid Films **292**, 14 (1997).
[13] S. A. Abd El-Hady, B. A. Mansour, and S. H. Moustafa, Phys. Status Solidi A **149**, 601 (1995).
[14] M. Leon, R. Diaz, F. Rueda, and M. Berghol, Sol. Energy Mater. Sol. Cells **26**, 295 (1992).
[15] J. E. Jaffe and A. Zunger, Phys. Rev. B **29**, 1882 (1984).
[16] S.-H. Wei and A. Zunger, Appl. Phys. Lett. **56**, 662 (1990).
[17] S.-H. Wei and A. Zunger, J. Appl. Phys. **76**, 3846 (1995).
[18] S. Shirakata, K. Murakami, and S. Isomura, Jpn. J. Appl. Phys., Part 1 **27**, 1780 (1988).
[19] S. Chichibu, Y. Harada, M. Uchida, T. Wakiyama, S. Matsumoto, S. Shirakata, S. Isomura, and H. Higuchi, J. Appl. Phys. **76**, 3009 (1994).
[20] S. Chichibu, H. Okumura, S. Nakamura, G. Feuillet, T. Azuhata, T. Sota, and S. Yoshida, Jpn. J. Appl. Phys., Part 1 **36**, 1976 (1997).